Search for a 17 keV Neutrino in the Electron-Capture Decay of ^{55}Fe

F. E. Wietfeldt,[1,2] Y. D. Chan,[1] M. T. F. da Cruz,[1,3] A. García,[1] R.-M. Larimer,[1] K. T. Lesko,[1] E. B. Norman,[1] R. G. Stokstad,[1] and I. Žlimen[1,a]

[1] *Nuclear Science Division, Lawrence Berkeley Laboratory, Berkeley, California 94720*

[2] *Physics Department, University of California, Berkeley, California 94720*

[3] *Physics Institute, University of São Paulo, São Paulo, Brazil*

(Received 13 November 1992)

Using a chemically purified sample of ^{55}Fe and a coaxial Ge detector, we collected a high-statistics internal-bremsstrahlung photon spectrum, and conducted a local search for departures from a smooth shape near the end point. We find no evidence for emission of a neutrino in the mass range 5–25 keV. In particular, a 17 keV neutrino with $\sin^2\theta = 0.008$ is excluded at the 7σ level.

PACS numbers: 23.40.Bw, 14.60.Gh, 27.40.+z

In extensions of the standard model with massive neutrinos, it is usual to let the neutrino weak eigenstates consist of superpositions of mass eigenstates in analogy to mass mixing in the quark sector. A two-state model of the electron neutrino is often considered:

$$|\nu_e\rangle = \cos\theta|\nu_1\rangle + \sin\theta|\nu_2\rangle\,, \tag{1}$$

where ν_1 and ν_2 are the mass eigenstates with masses m_1 and m_2, and θ is the mixing angle. We consider the case where $m_2 \gg m_1$ and θ is small. The observed nuclear β decay spectrum is a superposition of two spectra [1]

$$\frac{dN(E)}{dE} = \cos^2\theta\frac{dN(E, m_1 \approx 0)}{dE} + \sin^2\theta\frac{dN(E, m_2)}{dE}. \tag{2}$$

If this effect exists, it must be present in all β and electron capture (EC) decays where it is energetically allowed. It is convenient to express the total spectrum as [2]

$$\frac{dN(E)}{dE} \propto \frac{dN(E, m_\nu = 0)}{dE}S(E) \tag{3}$$

with

$$S(E) = 1 + \tan^2\theta\left[1 - \frac{m_2^2}{(Q-E)^2}\right]^{1/2} \tag{4}$$

for $E < Q - m_2$, and $S(E)$ equal to unity for $E \geq Q - m_2$. Q is the total decay energy. The experimental task is to determine if the function $S(E)$ is exhibited in the data. This function contains two main features: a sharp slope discontinuity (kink) at $E = Q - m_2$, and a difference in amplitude above and below the kink.

In 1985, Simpson reported a distortion in the tritium β decay spectrum which he interpreted to be the result of emission of a 17 keV neutrino [3]. In recent years several experiments have reported evidence of a 17 keV neutrino with $\sin^2\theta \approx 0.01$ in β decay and electron-capture internal-bremsstrahlung (IB) spectra [4–8]. The agreement in the results of these experiments is quite impressive. A number of other experiments, however, have not seen the effect [9–18]. A common feature of all the experiments (Ref. [15] excepted) is that in analyzing the data, a wide energy region is fit to the $m_\nu = 0$ theory and then compared to the same theory multiplied by $S(E)$. The values of m_2 and $\sin^2\theta$ which yield the lowest total χ^2 determine the result. Unfortunately, if a wide region is fit it is possible for an unexpected but smooth distortion in the spectrum to cause a lower χ^2 when $S(E)$ is included. Conversely, a smooth distortion can hide a neutrino kink in a similar way. A more effective test of the presence of a massive neutrino is to collect enough statistics to see the local slope discontinuity. It is unlikely that such a feature could be produced by anything other than a massive neutrino, and a local search for this kink should not be affected by smooth distortions.

It is well known that the second derivative of a spectrum can reveal the presence of γ-ray lines too small to be seen easily in the raw data [19]. We have found that the second derivative is also a powerful way to reveal the kink from a massive neutrino in a β or IB spectrum. The kink in $S(E)$ produces a bipolar peaklike structure in its second derivative. The size and shape of the structure depends on $\tan^2\theta$ and the detector resolution, and is insensitive to the shape of the underlying spectrum. The statistical dispersion of points in the second derivative of a spectrum is much larger than in the raw spectrum itself, so high statistics are needed to see the structure.

The EC decay of ^{55}Fe is an allowed ground-state to ground-state transition with a $Q_{\rm EC}$ value of 231.7 ± 0.7 keV, a probability of radiative EC, or IB, of 3.25×10^{-5}, and a half-life of 2.73 years [20]. In IB decay, the emitted photon and neutrino share the decay energy, producing a photon spectrum similar to a β spectrum. The theoretical IB spectrum for EC from the $1s$ shell is [21]

$$\frac{dN(E)}{dE} \propto E(Q_{\rm EC} - I - E)^2 R_{1s}(E). \tag{5}$$

The factor $R_{1s}(E)$ includes the most important relativistic and Coulomb effects, and I is the atomic excitation energy of the daughter ^{55}Mn atom. EC from higher shells produces a series of IB spectra with different end points superimposed on the dominant $1s$-capture spectrum.

A sample of ^{55}Fe was purchased from New England Nuclear Company. Initial γ-ray counting revealed impurities of ^{60}Co, ^{54}Mn, ^{123}Te, ^{127}Te, and ^{59}Fe, so we purified

the sample using an ion exchange column. The total EC strength of the purified source was about 25 mCi. The ^{55}Fe source was sealed inside a plastic container with 1-mm-thick walls and attached to the face of a 109-cm^3 coaxial Ge detector. An additional absorber, consisting of 0.06-mm-thick copper and 0.05-mm-thick aluminum foils, was placed between the source and detector to suppress the Mn x rays from the ^{55}Fe EC decays. The x-ray intensity was suppressed by a factor of about 3×10^6. The detector and source were placed inside an anticoincidence shield consisting of a 30-cm by 30-cm annular NaI detector and a 7.5-cm by 15-cm plug NaI detector. These NaI detectors were used to veto Compton-scattered events from the source and external background radiation. The initial ^{55}Fe IB counting rate in the Ge detector was approximately 8000 sec^{-1}.

Three separate spectra were recorded simultaneously on three Ortec 916A analog-to-digital converters (ADCs): (A) Ge detector with no vetos, (B) Ge detector with pileup rejection (PUR) using the pileup inhibit veto from an Ortec 572 amplifier, and (C) Ge detector with PUR and NaI veto. The PUR and NaI veto thresholds were measured to be 27.0 and 29.5 keV, respectively. The spectra with PUR contain residual pileup caused by photons detected too close together in time to be vetoed. This residual pileup is referred to below as the pileup spectrum. A total of 145 days of ^{55}Fe data were collected in 2–3 day intervals on a PC based acquisition system. The energy scale was calibrated using Pb x rays and ^{59}Fe lines in the spectra, and verified with external calibration γ-ray sources. Background spectra were accumulated between ^{55}Fe measurements. Separate sources of ^{59}Fe, ^{60}Co, and ^{54}Mn were also measured. All lines in the background and ^{55}Fe spectra (50–400 keV) were identified and accounted for by normal room background and the above-mentioned impurities. As a result of time variations in the peak to continuum ratio of the background in the environment of the experiment, we were unable to simultaneously normalize the peak and continuum areas of the background spectra to the ^{55}Fe spectra. Normalizing on the peaks leaves a residual continuum of approximately 2000 counts/channel, which is about 0.1% of the total at 208 keV. This is not expected to affect the results of our analysis, but as a precaution the background was normalized in two ways, first on the peaks and then on the continuum in the region 420–500 keV. The complete analysis was performed on both data sets, with virtually identical results. The results presented here were obtained using the peak-normalized background subtracted data. After subtracting background and impurity lines, ^{55}Fe spectrum C contained 1.13×10^7 counts/keV at 208 keV (the 1s-capture kink position for a 17 keV neutrino). ADC nonlinearities were measured with a ramp pulser. The ADC used to collect ^{55}Fe spectrum C had a differential nonlinearity of less than 0.2% and an integral nonlinearity of 1% in the energy region 130–260 keV. Figure 1 shows the total raw data in ^{55}Fe spectrum C and the peak-normalized background and impurity spectra.

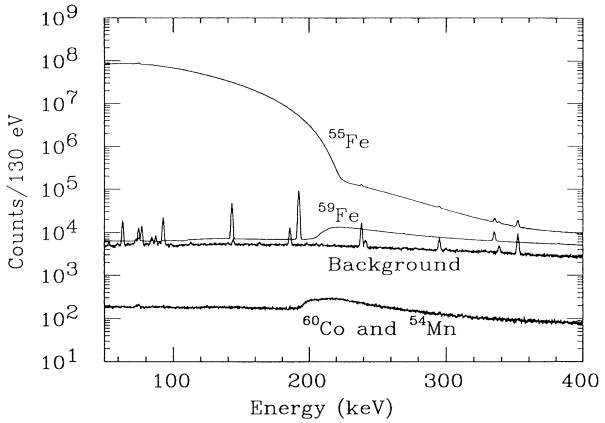

FIG. 1. The total raw data collected in spectrum C, with pileup rejection and NaI veto. Also shown are the peak-normalized background and impurity spectra.

In order to test the effectiveness of the analysis methods, a Monte Carlo program was developed to generate spectra simulating ^{55}Fe spectrum C. The theoretical IB spectra were calculated for EC from the 1s and 2s states using the relativistic theory of Glauber and Martin [21,22], and from the 2p and 3p states using the theory of De Rújula [23]. A value of $Q_{\rm EC} = 231.0$ keV gave the best match to the actual ^{55}Fe data. The photon response of the detector was measured using test sources of ^{241}Am, ^{57}Co, ^{139}Ce, and ^{203}Hg, in a similar source geometry and with the same veto conditions as ^{55}Fe spectrum C. The photopeak resolution at 208 keV was approximately 1.3 keV FWHM. The detector response model consisted of a Gaussian photopeak, a flat tail approximating the suppressed Compton response, and a small triangular peak corresponding to photons that Compton backscattered in the Ge detector cold finger and thus avoided the NaI veto. The model was parametrized by simple functions in energy using the test source data. The detector photopeak efficiency was measured using test sources, and fit to a standard functional form [24]. We also applied a correction factor equal to $[1 + 0.0008(E_0 - E)]$, where E_0 is the end point energy in keV, to the calculated spectrum to correct for a linear divergence from the actual data. We attribute this divergence to systematic uncertainty in measuring the photopeak efficiency at such close geometry, and we emphasize that this type of correction will not affect a local search for a kink in the spectrum. Finally, the pileup rejection efficiency of the Ortec 572 amplifier was measured using the ^{55}Fe source and an Ortec 467 time-to-amplitude converter (TAC). This was combined with a self-convolution of the calculated spectrum to generate the pileup spectrum. Poisson statistics were then applied to the total calculated spectrum. The second derivative of a Monte Carlo spectrum, including a 1% ($\sin^2\theta = 0.01$) 17 keV neutrino and generated with infinite statistics, is shown in Fig. 2(a) (solid curve) illus-

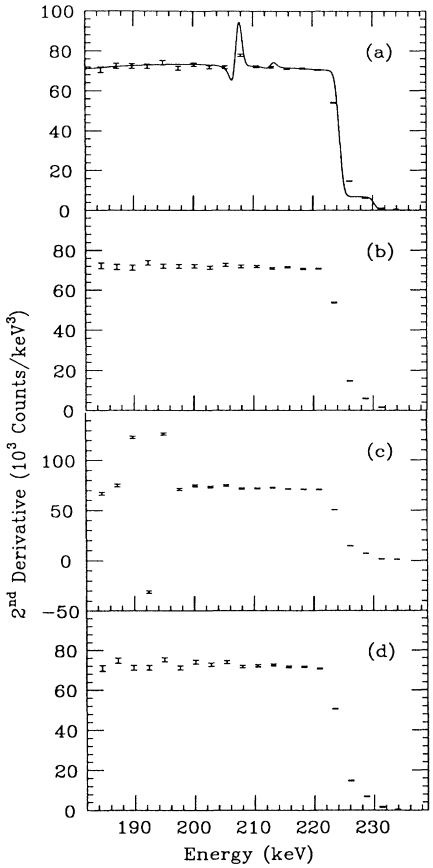

FIG. 2. Second derivatives of Monte Carlo spectra generated with (a) a 1% 17 keV neutrino and (b) no massive neutrino. The statistics are equivalent to those of ^{55}Fe spectrum C. Also shown in (a) is the second derivative of a Monte Carlo spectrum with infinite statistics (solid curve) generated with a 1% 17 keV neutrino. The structures at 208 and 214 keV are due to massive neutrino emission in the 1s- and 2s-capture decays, respectively. Second derivatives of ^{55}Fe spectrum C (c) before background and impurity subtraction (revealing the ^{59}Fe line at 192 keV) and (d) after background and impurity subtraction.

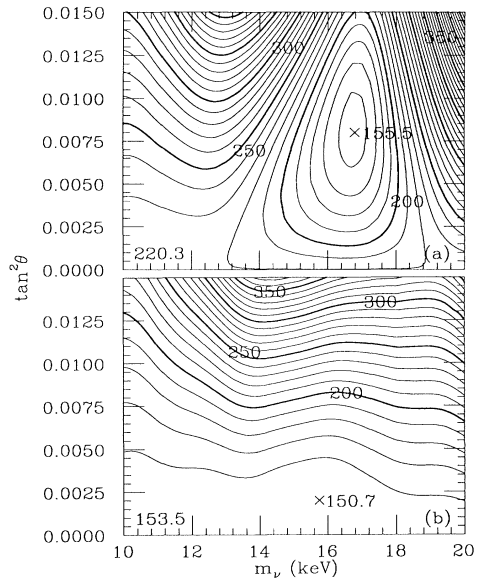

FIG. 3. χ^2 contours for polynomial fits to Monte Carlo data with (a) a 1% 17 keV neutrino and (b) no massive neutrino. The region fit is 200–220 keV in 130-eV-wide bins (154 data points). The absolute minima are marked with an X.

trating the structure produced by the massive neutrino. There are two visible kinks, one at 208 keV from the 1s-capture spectrum and one at 214 keV from the 2s-capture spectrum.

Figure 2(a) also shows the second derivative of a Monte Carlo spectrum generated with a 17 keV neutrino and $\sin^2\theta = 0.01$, with statistics equivalent to the experimental data. A peak is clearly visible at 208 keV. Figure 2(b) shows the second derivative of a Monte Carlo spectrum with no massive neutrino. Both spectra were generated in 130-eV-wide bins with 1.13×10^7 counts/keV at 208 keV (matching ^{55}Fe spectrum C), and compressed into twenty channel bins (2.6 keV/bin) to reduce the statistical variation of the points. Figure 2(c) shows the second derivative of ^{55}Fe spectrum C raw data. The structure at 188–196 keV is due to a 192 keV γ-ray line from the ^{59}Fe impurity. Figure 2(d) shows the same spectrum after subtraction of the background and impurity lines. There is no sign of a 17 keV neutrino kink. To ensure that the data compression did not hide the kink, twenty versions of each binned spectrum were generated, each with twenty channels per bin but with different channel offsets. None of these spectra show evidence of a massive neutrino kink. Second derivatives of ^{55}Fe spectra A and B also show no neutrino kinks.

We do not attempt to quote a strict confidence level based directly on the second derivative results. A traditional χ^2 fit to the theory would be complicated by the covariance in adjacent points of the second derivative. Instead we performed an additional analysis of the data. If no kinks are present we expect a narrow region of the ^{55}Fe spectrum to be smooth, and well fit by a low-order polynomial. If a kink corresponding to emission of a massive neutrino is present in the region, it should be well fit by this polynomial multiplied by $S(E)$. The following function was used in fitting the data:

$$P(E) = (a_0 + a_1E + a_2E^2 + a_3E^3)S'(E)\,, \qquad (6)$$

where $S'(E)$ is $S(E)$ convoluted by a pure Gaussian with a width corresponding to the measured detector response. For each fit, m_2 and $\tan^2\theta$ were fixed and a_0–a_3 were varied freely to minimize χ^2. Because the presence of a pileup spectrum will slightly dilute the effect of the kink, the analysis was performed on Monte Carlo data generated with and without pileup, and on the actual data both with and without pileup. The pileup was removed

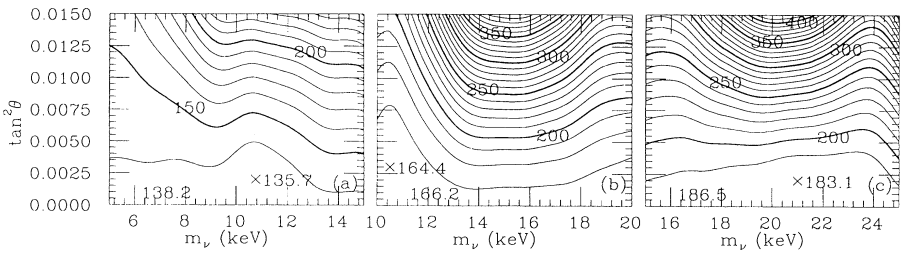

FIG. 4. χ^2 contours for polynomial fits to ^{55}Fe spectrum C with 130-eV-wide bins in the regions (a) 205–224 keV (147 data points), (b) 200–220 keV (154 data points), and (c) 195–215 keV (154 data points). The absolute minima are marked with an X.

from the data by normalizing the theoretical pileup spectrum to the data at 235 keV and subtracting.

Figure 3(a) shows the χ^2 contours for fits to Monte Carlo data generated with a 1% 17 keV neutrino, in the region 200–220 keV, in 130-eV-wide bins (154 data points), and with no pileup. The χ^2 minimum corresponds to a neutrino of mass 16.8 ± 0.4 keV with $\tan^2\theta = 0.008 \pm 0.001$ (1σ). The mixing is slightly low due to the presence of the 2s-capture IB spectrum, which contributes 15% of the total at 208 keV, and dilutes the strength of the 1s-capture kink. Figure 3(b) shows a similar plot for Monte Carlo data generated in the same way but with no massive neutrino.

Three different regions of ^{55}Fe spectrum C were fit to different ranges of neutrino mass: 195–215 keV with m_2=15–25 keV (154 points); 200–220 keV with m_2=10–20 keV (154 points); and 205–224 keV with m_2=5–15 keV (147 points). Figure 4(b) shows the χ^2 contours for the fits of the 200–220 keV region. The best fit is $m_2 = 10.5$ keV and $\tan^2\theta = 0.003$, with $\chi^2 = 164.4$ ($\chi^2_\nu = 1.10$), which is statistically consistent with no massive neutrino ($\chi^2 = 166.2$). A 0.8% 17 keV neutrino should give $\tan^2\theta = 0.007$ after correcting for the 2s IB spectrum. This yields $\chi^2 = 212.5$, a difference of 48.1 units (6.9σ) from the minimum. Figures 4(a) and 4(c) show the χ^2 contours for the fits of the other two regions. There is no evidence for massive neutrino emission in either region. Similar analyses of ^{55}Fe spectrum C without pileup subtraction and ^{55}Fe spectra A and B exclude a 0.8% 17 keV neutrino by 6.7σ, 5.8σ, and 5.5σ, respectively. Finally, to verify that this analysis would not be affected by a smooth distortion in the spectrum, Monte Carlo spectra were generated with arbitrarily chosen linear and quadratic factors, with and without massive neutrinos; and these spectra were analyzed in the same way. The presence or absence of a neutrino kink was always correctly found.

As a result of the Monte Carlo tests performed, we conclude that this experiment was sensitive to the local effect of a kink in the ^{55}Fe IB spectrum caused by the emission of a massive neutrino in a small fraction of decays. Analysis of the actual data showed no evidence of this kink. Thus we conclude that the effect reported previously in lower statistics experiments, and interpreted to be the result of a 17 keV neutrino, is not in fact caused by a massive neutrino.

We wish to thank M. M. Hindi for helpful discussions. This work was supported by the Nuclear Physics Division of the U.S. Department of Energy under Contract No. DE-AC03-76SF00098, and by Fundação de Amparo à Pesquisa do Estado de São Paulo, FAPESP, São Paulo, Brazil.

[a] On leave from R. Bošković Institute, Zagreb, Croatia.

[1] F. Boehm and P. Vogel, *Physics of Massive Neutrinos* (Cambridge Univ. Press, Cambridge, 1987), p. 68.
[2] A. Hime, Mod. Phys. Lett. A **7**, 1301 (1992).
[3] J.J. Simpson, Phys. Rev. Lett. **54**, 1891 (1985).
[4] J.J. Simpson and A. Hime, Phys. Rev. D **39**, 1825 (1989).
[5] A. Hime and J.J. Simpson, Phys. Rev. D **39**, 1837 (1989).
[6] A. Hime and N.A. Jelley, Phys. Lett. B **257**, 441 (1991).
[7] B. Sur *et al.*, Phys. Rev. Lett. **66**, 2444 (1991).
[8] I. Žlimen *et al.*, Phys. Rev. Lett. **67**, 560 (1991).
[9] T. Ohi *et al.*, Phys. Lett. **160B**, 322 (1985).
[10] V.M. Datar *et al.*, Nature (London) **318**, 547 (1985).
[11] T. Altzitzoglou *et al.*, Phys. Rev. Lett. **55**, 799 (1985).
[12] A. Apalokov *et al.*, Pis'ma Zh. Eksp. Teor. Fiz. **42**, 233 (1985) [JETP Lett. **42**, 289 (1985)].
[13] J. Markey and F. Boehm, Phys. Rev. C **32**, 2215 (1985).
[14] D.W. Hetherington *et al.*, Phys. Rev. C **36**, 1504 (1987).
[15] H. Kawakami *et al.*, Phys. Lett. B **287**, 45 (1992).
[16] M. Bahran and G. Kalbfleisch, Phys. Lett. B **291**, 336 (1992).
[17] J.L. Mortara *et al.*, Phys. Rev. Lett. **70**, 394 (1993).
[18] D.E. DiGregorio *et al.*, Phys. Rev. C (to be published).
[19] M.A. Mariscotti, Nucl. Instrum. Methods **50**, 309 (1967).
[20] E. Browne and R.B. Firestone, *Table of Radioactive Isotopes* (Wiley, New York, 1986).
[21] W. Bambynek *et al.*, Rev. Mod. Phys. **49**, 77 (1977).
[22] R.J. Glauber and P.C. Martin, Phys. Rev. **104**, 158 (1956); P.C. Martin and R.J. Glauber, Phys. Rev. **109**, 1307 (1958).
[23] A. De Rújula, Nucl. Phys. **B188**, 414 (1981).
[24] G.F. Knoll, *Radiation Detection and Measurement* (Wiley, New York, 1989), p. 459.